Enhanced mineralization of hypersaline wastewater with Fe^{2+}/Cu^{2+} catalyzed UV-Fenton process: process optimization and catalytic mechanism

Xiaofang Yang, Zhaoyi Yang, Zhen Liu, Weijun Zhang and Dongsheng Wang

ABSTRACT

The efficiency of Fenton oxidation was inhibited by the high content of salt in the industrial wastewater. However, enhanced mineralization of hypersaline industrial wastewater is necessary for advanced treatment and subsequent wastewater salt recovery process. Therefore, Fe^{2+} and Cu^{2+} catalyzed UV-Fenton oxidation were carried out to improve the total organic carbon (TOC) removal efficiency for a hypersaline wastewater from resin manufacturing. The performance of UV-Fe/Cu-Fenton oxidation was comparatively investigated and optimized using response surface methodology (RSM) to develop a practical high-efficient mineralization treatment technique for hypersaline wastewater. More than 90% of TOC was removed under optimal conditions of UV-Fe^{2+} and UV-Cu^{2+}-Fenton oxidation, namely 9.6 mM Fe^{2+} and 176 mM H_2O_2, and 2.95 mM Cu^{2+} and 276 mM H_2O_2, respectively. The reactive oxygen radicals identified using electron spin resonance (ESR) spectroscopy revealed that hydroxyl radical was dominant oxidant in UV-Fe^{2+}-Fenton process, while $HO_2\cdot/O_2\cdot^-$ played a more important role in the UV-Cu-Fenton system. The Cl^- effect is also different for UV Fe and Cu Fenton. Moreover, no scaling and sludge problem makes UV-Cu-Fenton a promising alternative method for efficient mineralization of hypersaline industrial wastewater.

Key words | copper(II), hypersaline wastewater, mineralization, radicals, UV-Fenton

Xiaofang Yang
Zhaoyi Yang
Dongsheng Wang (corresponding author)
State Key Laboratory of Environmental Aquatic Chemistry, Research Centre for Eco-Environmental Sciences,
Chinese Academy of Sciences,
Beijing 100085,
China
E-mail: *wgds@rcees.ac.cn*

Zhen Liu
Weijun Zhang
Dongsheng Wang
School of Environmental Studies,
China University of Geosciences,
Wuhan 430074, Hubei,
China

INTRODUCTION

Industrial wastewater with high organic content and salinity is a big challenge for biological treatment systems without pre-treatment. For instance, the chemical oxygen demand (COD) of wastewater discharged from epoxy resin and epoxy chloropropane manufacturing is higher than 10,000 mg/L and the NaCl concentration is higher than 20% w/v. Using conventional pre-dilution and biodegradation processes for high saline wastewater treatment, not only consume large amount of fresh water and increase the discharge load of secondary waste water, but also lose valuable mineral salt resource. Accordingly, when salt recycling is of a major consideration, enhanced total organic carbon (TOC) removal is important in the wastewater treatment. That is because the currently used salt concentration techniques, such as multiple effect evaporation (MEE) or membrane electrolysis, require low organic content of the influent water. Therefore, advanced treatment and enhanced mineralization of hypersaline industrial wastewater is very imperative and provide a possibility for salt resources recovery from the wastewater.

Fenton oxidation technique is one of the most commonly used advanced oxidation processes (AOPs) for mineralization treatment of hazardous and/or biorefractory wastewater (Teel *et al.* 2001; Pignatello *et al.* 2006; Wang & Xu 2012). It is well known that Fenton process is dependent on non-selective radicals-HO· which are formed as described by Equations (1) and (2), and the efficiency of conventional Fenton oxidation on organics removal is largely inhibited by inorganic ions such as chloride and sulfate ions (Lipczynskakochany *et al.* 1995; Pignatello *et al.* 2006). Chloride ions could act as the scavengers of HO· and form chlorine radicals which are less reactive than ·OH (Pignatello 1992), as shown in Equations (3)–(5). Chloride ions are also able to form complexes with Fe^{2+}/Fe^{3+}

doi: 10.2166/wst.2018.390

(Equations (6)–(8)), thus decreasing the reaction rate of Fe species with H_2O_2 (De Laat *et al.* 2004).

Extensive studies have shown that addition of external photo energy could enhance the oxidative degradation and mineralization of pollutants by Fenton reaction (Pignatello 1992; Wei *et al.* 2011; Wang & Xu 2012; Wu *et al.* 2016). It has been reported that the effect of NaCl on the mineralization of synthetic phenol wastewater by UV-Fenton reaction was insignificant at low NaCl concentration, and the mineralization was only moderately inhibited at high NaCl concentration (>50 g/L) (Maciel *et al.* 2004). In UV assisted Fenton oxidation, the reduction of Fe(III) species to Fe(II) (Equations (9)–(11)) were accelerated (Pignatello *et al.* 2006; Giri & Golder 2014). Therefore, UV assisted Fenton oxidation could be used for the TOC removal of hypersaline resin processing wastewater which is colorless and relatively low turbidity. However, the reaction conditions and organics degradation performance need to be optimized for practical application in the treatment of high saline wastewater.

$$Fe^{2+} + H_2O_2 \rightarrow Fe^{3+} + \cdot OH + OH^- \quad (1)$$

$$Fe^{3+} + H_2O_2 \rightarrow Fe^{2+} + HO_2\cdot + H^+ \quad (2)$$

$$\cdot OH + Cl^- \rightarrow HOCl\cdot^- \quad (3)$$

$$HOCl\cdot^- + H^+ \rightarrow Cl\cdot + H_2O \quad (4)$$

$$Cl\cdot + Cl^- \rightarrow Cl_2\cdot^- \quad (5)$$

$$Fe^{3+} + Cl^- \rightarrow FeCl^{2+} \quad (6)$$

$$Fe^{3+} + 2Cl^- \rightarrow FeCl_2^+ \quad (7)$$

$$Fe^{2+} + Cl^- \rightarrow FeCl^+ \quad (8)$$

$$Fe(OH)^{2+} + h\nu \rightarrow Fe^{2+} + HO\cdot \quad (9)$$

$$Fe^{3+}(L)_n + h\nu \rightarrow Fe^{2+}(L)_{n-1} + L_{ox} \quad (10)$$

$$FeCl^{2+} + h\nu \rightarrow Fe^{2+} + \cdot Cl^- \quad (11)$$

Besides Fe ions, Cu is also an active transition metal which shows hydrogen peroxide activation ability (Equations (12) and (13)) (Nieto-Juarez *et al.* 2010; Bokare & Choi 2014). Copper ions ($Cu^{2+/+}$) have similar redox properties as iron ions ($Fe^{3+/2+}$) but different solubility and complexation characteristics, resulting in a different behavior of $Cu^{2+/+}$ in Fenton-like reaction. $Cu^{2+/+}$ shows a faster H_2O_2 reaction rate than $Fe^{3+/2+}$ species and could be carried out under more neutral conditions, since the cupric aqua species are more soluble at neutral pH (Bokare & Choi 2014; Peng *et al.* 2016). However, copper was seldom used in homogeneous Fenton oxidation due to the instability of Cu^+ and the higher cost of copper salt and potential toxicity of residue copper ions in effluent. Nevertheless, it has been found that UV radiation could also enhance the Cu ions catalyzed Fenton-like oxidation (Nerud *et al.* 2001; Salazar *et al.* 2012). However, the performance of Cu-Fenton oxidation of saline wastewater and the catalytic mechanism were still not clearly understood.

$$Cu^{2+} + H_2O_2 \rightarrow Cu^+ + HO_2\cdot + H^+ \quad (12)$$

$$Cu^+ + H_2O_2 \rightarrow Cu^{2+} + \cdot OH + OH^- \quad (13)$$

Therefore, the purposes of this work were to: (a) comparatively evaluate the performance of UV assisted Fe-Fenton and Cu-Fenton for organic pollutants removal from hypersaline wastewater; (b) optimize the mineralization efficiency using response surface methodology (RSM) and develop a practical high-efficient mineralization treatment technique for actual hypersaline wastewater; (c) elucidate the catalytic mechanisms involved in the Fe^{2+} and Cu^{2+} catalyzed UV-Fenton process.

MATERIALS AND METHODS

Materials

The industrial wastewater samples were taken from an epoxy resin manufacturer in Jiangsu Province, China. The wastewater samples contain mainly glycerin, NaCl, bisphenol A diglycidyl ether and epoxy chloropropane. Raw wastewater and water samples after primary Fenton oxidation on site were taken. About 55% of COD and 8% TOC were removed by the primary Fenton oxidation, but the water quality was not good enough for further salt recovery using membrane electrolysis technique. The UV-visible spectra of the wastewater before and after primary Fenton oxidation are given in supporting information (Figure S1 in the Supplementary Material, available with the online version of this paper). The characteristics of the wastewater sample are given in Table S1 (available online). The present study was carried out using the pre-treated samples as advanced treatment in order to further enhance the TOC removal of the wastewater.

All chemicals used are analytical grade reagents. Hydrogen peroxide (30% w/w), ferrous sulfate ($FeSO_4\cdot 7H_2O$), $Cu(NO_3)_2\cdot 3H_2O$, HCl and NaOH were purchased from Sinopharm Chemical Reagent Co. Ltd. 5,5-Dimethyl-1-pyrroline-N-oxide (DMPO) used in electron spin resonance (ESR) experiments

were supplied by J&K Scientific Ltd. Ultrapure water (Milli-Q) was used to prepare solutions.

Experimental procedure

UV-Fenton oxidation procedure

The Fenton reagents were added into the wastewater sample to start the reaction in a single dose or continuous dosing by peristaltic pump in an experimental setup as in Figure S2 (available online). In the optimization experiments of oxidation process conditions, lamps with various powers were used as described in the data. The pH and temperature of solution were measured during the reaction. At given time intervals, a small aliquot was sampled and added with excess of NaOH to quench the reaction. After immediate centrifugation, the supernatant was collected for analysis. All experimental runs were performed in duplicate at ambient temperature unless indicated otherwise.

Analysis methods

TOC and UV absorbance of water sample was measured using TOC-Vcph analyzer (Shimadzu, Japan) and UV-Vis spectrophotometer (U-2910, Hitachi, Japan), respectively. H_2O_2 concentration was measured using titanium sulfate method (Eisenberg 1943). The species of radicals in the filtrate of the reaction solution were identified using 5,5-Dimethyl-1-pyrroline N-oxide (DMPO) as trapping agent by ESR spectroscopy (Bruker model ESP 300E). The ESR spectroscopy was operated at 3514 G center field and 9.85 GHz microwave frequency.

Response surface methodology (RSM) experimental design

The process optimization was carried out using a Box-Behnken design with three factors and three coded levels experimental design (Design Expert 8.0). The dosages of H_2O_2 (X_1) and Fe(II) salt or Cu(II) salt (X_2) and power of UV lamp (X_3) were chosen as independent input variables. The TOC removal efficiency was used as the dependent output variable (y). The response variable was fitted by a quadratic polynomial equation

$$y = b_0 + \sum_{i=1}^{3} b_i X_i + \sum_{i=1}^{3} b_{ii} X_{ii}^2 + \sum_{i=1}^{2} \sum_{j=i+1}^{3} b_{ij} X_i X_j \quad (14)$$

where y represents the predicted TOC removal rate of wastewater sample after oxidation, b_0, b_i and b_{ij} are the fitted coefficients, X_i and X_j are the code values of the independent variables. The experimental range and coded levels of the variables are listed in Table S1 in the supporting information.

RESULTS AND DISCUSSION

TOC removal and H_2O_2 decomposition in UV-Fe/Cu-Fenton oxidation

Figure 1(a) shows the TOC removal efficiency with time in different oxidation processes catalyzed by Fe^{2+} or Cu^{2+} ions. After 100 min reaction, the TOC was reduced to 85, 68 and 22 mg/L for Fe-Fenton, UV-Fe-Fenton and

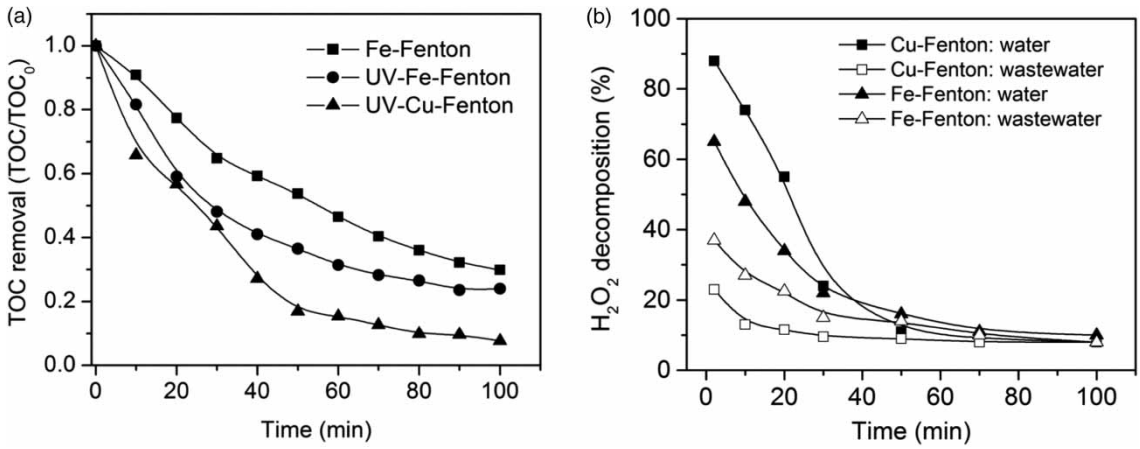

Figure 1 | (a) UV enhanced TOC removal ($[Fe^{2+}]_0 = [Cu^{2+}]_0 = 0.0167$ mol/L, $[H_2O_2]_0 = 0.5$ mol/L) and (b) H_2O_2 decomposition ($[Fe^{2+}]_0 = [Cu^{2+}]_0 = 0.01$ mol/L, $[H_2O_2]_0 = 0.3$ mol/L) in UV Fe/Cu-Fenton oxidation processes.

UV-Cu-Fenton systems, respectively. UV irradiation could significantly promote the Fenton oxidation rate and mineralization of pollutants as expected. In addition, UV assisted Cu-Fenton system shows a better TOC removal than Fe-Fenton system. This is partly due to the reactive radicals generation rates in the Cu^{+}/Cu^{2+}-H_2O_2 reactions (Equations (12) and (13)) are several orders of magnitude higher than Fe^{2+}/Fe^{3+} catalyzed reactions (Equations (1) and (2)) (Moffett & Zika 1987; Bokare & Choi 2014). The kinetic rate constants for reaction in Equations (1), (2) and (12), (13) are 40–80 $(mol/L)^{-1}\cdot s^{-1}$, 2×10^{-3} $(mol/L)^{-1}\cdot s^{-1}$, and 4.6×10^{2} $(mol/L)^{-1}\cdot s^{-1}$, 1×10^{4} $(mol/L)^{-1}\cdot s^{-1}$ (Moffett & Zika 1987; Salazar *et al.* 2012). The photo-induced reduction of $Fe(OH)^{2+}$ to Fe^{2+} and generation of HO· (Equations (9)–(11)) contributed to the promoted TOC removal (Maciel *et al.* 2004; Machulek *et al.* 2007). With the presence of high concentration of Cl^{-} ions, the photolysis of Fe(III)-complexes such as $FeCl^{2+}$ to Fe^{2+} and Cl· increased the reduction of Fe(III) species to Fe(II) compared to non-irradiated process (Nadtochenko & Kiwi 1998). Similarly, in the UV-Cu-Fenton reaction, the reduction of Cu(II) species with H_2O_2 was increased due to the photo-reactivity of the formed Cu(II)-Cl and Cu-organic ligand complexes (Millero *et al.* 1992).

As shown in Figure 1(b), H_2O_2 was decomposed rapidly in the first 30 min in all the systems. In pure water medium, the decomposition of H_2O_2 by Cu ions was slower than by the Fe ions possibly due to the oxidation of Cu(I) by oxygen (Gallard *et al.* 1999). With the presence of organic pollutants, the decomposition of H_2O_2 increased significantly than in the pure water medium, especially for Cu^{2+}-H_2O_2 system. More than 70% of H_2O_2 was decomposed by Cu^{2+} in the first 1 min of reaction. The complexes of Fe with degradation intermediates are more stable and less reactive with H_2O_2 than Cu complexes, leading to a lower TOC removal efficiency of UV-Fe-Fenton than UV-Cu-Fenton (Millero *et al.* 1992; Nerud *et al.* 2001; Lan *et al.* 2016). About 90% of H_2O_2 was decomposed in the wastewater sample after 30 min of reaction for both Cu and Fe catalytic systems. However, the TOC unceasingly reduced about 30% in UV-Cu-Fenton oxidation and 20% in UV-Fe-Fenton oxidation after 30 min of reaction when most of the H_2O_2 was consumed.

Effects of reagent dosing manner and pH in UV-Fe-Fenton

The TOC removal efficiency varied with concentration of Fe^{2+} and reagent dosing manners (Figure S3 in Supplementary Material, available with the online version of this paper). The TOC removal rate was increased with increased Fe^{2+}: H_2O_2 molar ratio from 1:30 to 1:20, and reduced at 1:10 with fixed H_2O_2 dosage. Excess amount of Fe^{2+} ions and H_2O_2 both will consume the generated HO· and $HO_2\cdot$/ $O_2\cdot^{-}$ (Equations (15)–(18)). In fact, it is the actual concentration, instead of the dosage, of Fe^{2+} and H_2O_2 determines the kinetics and affect the performance of Fenton reaction in the process.

$$Fe^{2+} + \cdot OH \rightarrow Fe^{3+} + OH^{-} \quad (15)$$

$$Fe^{2+} + HO_2\cdot + H^{+} \rightarrow Fe^{3+} + H_2O_2 \quad (16)$$

$$\cdot OH + H_2O_2 \rightarrow HO_2\cdot + H_2O \quad (17)$$

$$HO_2\cdot + HO_2\cdot \rightarrow H_2O_2 + O_2 \quad (18)$$

Compared with single dose of reagent (Figure S3), the continuous dosing of Fenton's reagent was benefit for the reaction by lowering the instantaneous concentration of Fe^{2+} and H_2O_2 at the initial stage of the reaction and sustaining the generation of HO·. Therefore, the continuous dosing manner was used for both Fe and Cu-Fenton system in order to obtain a better TOC removal efficiency.

pH is an important factor for Fenton reaction by determining the iron species distribution (Pignatello *et al.* 2006). Normally, pH between 3 and 4 is optimal for Fe-Fenton reaction (Tang & Huang 1996; Duesterberg & Waite 2006). It was noted that pH of reaction medium was always declined in wastewater treatment due to hydrolysis of ferric ions and formation of organic intermediates, such as formic acid and acetic acid. Results in Figure 2(a) reveal that keep the pH at 3 is beneficial for TOC removal, which is in accordance with literature (Tang & Huang 1996; Duesterberg & Waite 2006). Without pH control, the pH of the solution decreased to pH 2, and the corresponding TOC removal was about 86% after 100 min of reaction (Figure 2(a)). However, when the pH was maintained at 3, a maximum 96% TOC removal was achieved at 50 min (Figure 2(a)). Therefore, to get a better TOC removal using the Fe catalyzed Fenton, particular attention needs to be paid on continual control of pH throughout the process.

However, for the Cu-Fenton reaction, the final pH dropped to 3 without pH control and the TOC removal efficiency still reached 90% after 90 min (Figure 2(b)). The Cu-Fenton is less sensitive to pH and could be carried out in near neutral pH range due to the Cu^{2+} species are more soluble at higher pH than Fe^{3+} (Millero *et al.* 1992; Peng *et al.* 2016). Therefore, for UV-Cu-Fenton oxidation, pH control was less important compared with Fe-Fenton oxidation.

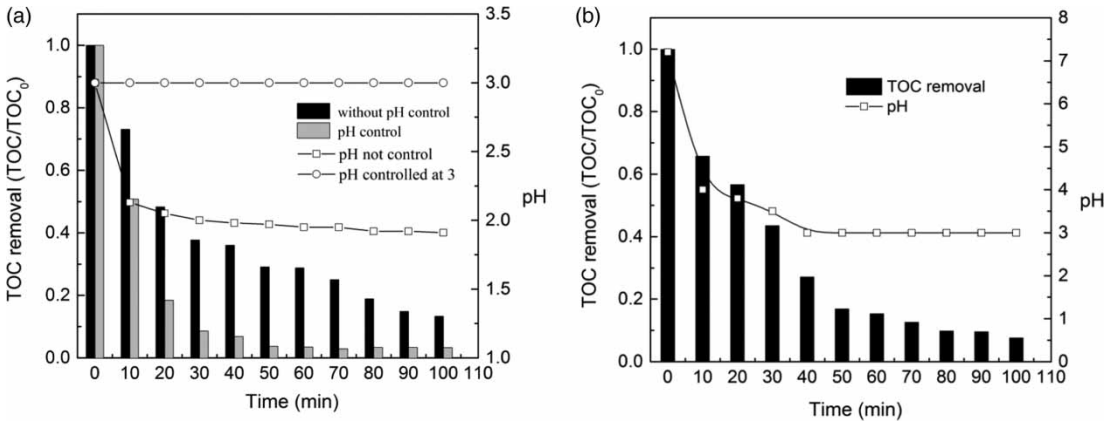

Figure 2 | Effects of pH on TOC removal in (a) UV-Fe-Fenton and (b) UV-Cu-Fenton (no pH control). Columns, the TOC removal efficiency under different pH conditions; lines with scatters, the variation of pH during reaction; $[Fe^{2+}]_0 = 0.025$ mol/L, $[Cu^{2+}]_0 = 0.017$ mol/L, $[H_2O_2]_0 = 0.5$ mol/L, the Fenton's reagent was dosed continuously.

Optimization of reaction conditions of UV-Fe/Cu-Fenton oxidation using response surface methodology (RSM)

RSM was used to optimize the reaction conditions for UV-Fe-Fenton and UV-Cu-Fenton systems. A Box–Behnken design with three factors and three coded levels experimental design was used, and a total of 17 batch experiments were carried out for each system to develop the response surface model (Table S2, available online). Equations (19) and (20) show the fitted quadratic polynomial model in terms of coded variables for UV-Fe-Fenton and UV-Cu-Fenton system, respectively. The obtained TOC removal efficiencies varied between 26% to 96% for UV-Fe-Fenton system and 62% to 91% for UV-Cu-Fenton system, and the predicted values were in good agreement with the experimental observations.

$$y = 78.32 + 18.93X_1 - 3.35X_2 + 14.43X_3 + 7.69X_1X_2 - 5.67X_1X_3 + 6.91X_2X_3 - 15.93 \quad (19)$$

$$y = 74.60 + 8.84X_1 - 7.12X_2 + 1.53X_3 - 3.13X_1X_2 - 0.19X_1X_3 - 0.12X_2X_3 - 2.96X_1^2 + 1.98X_2^2 + 5.54X_3^2 \quad (20)$$

where y is the predicted TOC removal, X_1 is the dosage of H_2O_2 coded values, X_2 is the concentration of ferrous sulfate or copper nitrate coded values, X_3 is the power of UV lamp.

The analysis of variance (ANOVA) results for UV-Fe/Cu-Fenton systems are summarized in Table S3 in the Supplementary Material (available online). The quality of the fitting was expressed by the correlation coefficient R^2, which is 0.9767 for UV-Fe-Fenton and 0.9882 for UV-Cu-Fenton, suggesting that 97.67% and 98.83% of total variation could be explained by the model, respectively. The model P value calculated from ANOVA analysis indicated that the derived regression model is significant for TOC removal in both Fe- and Cu-Fenton systems. Therefore, the derived model is adequate for prediction and optimization of the reaction conditions of the UV-Fenton reaction.

The significance of each independent variable was evaluated using the calculated P value, as denoted in Table S3. The results indicate that for the Fe-Fenton system, the TOC removal of the studied hypersaline wastewater is significantly affected by H_2O_2 concentration and the intensity of UV irradiation and the Fe concentration has a relatively minor effect. For the UV-Cu-Fenton system, all the three variables are significant, and Cu^{2+} and H_2O_2 concentration are more important factors for the TOC removal. The interactive relationships of independent variables and response value were presented in Figure 3 and Figures S4 and S5 (available online).

The maximum profile of surface response for UV-Fe-Fenton indicates that the TOC removal efficiency could be improved by increasing the intensity of UV irradiation when the H_2O_2 concentration was less than about 200 mM (Figure S4). The interaction between concentration of Fe^{2+} and H_2O_2 on TOC removal suggests that at low concentration of H_2O_2, the increase of Fe^{2+} concentration could not improve the TOC removal and the maximum TOC removal was obtained at H_2O_2 concentration about 200 mM (Figure 3(a)).

For the UV-Cu-Fenton system, unlike the Fe-Fenton system, the interaction between UV irradiation and H_2O_2 concentration or Cu^{2+}concentration is insignificant (Table S3 and Figure S5), implying a different mechanism for UV-Cu-Fenton reaction than UV-Fe-Fenton. Figure 3(b) shows that higher TOC removal was obtained at lower Cu^{2+} concentration and higher H_2O_2 concentration at

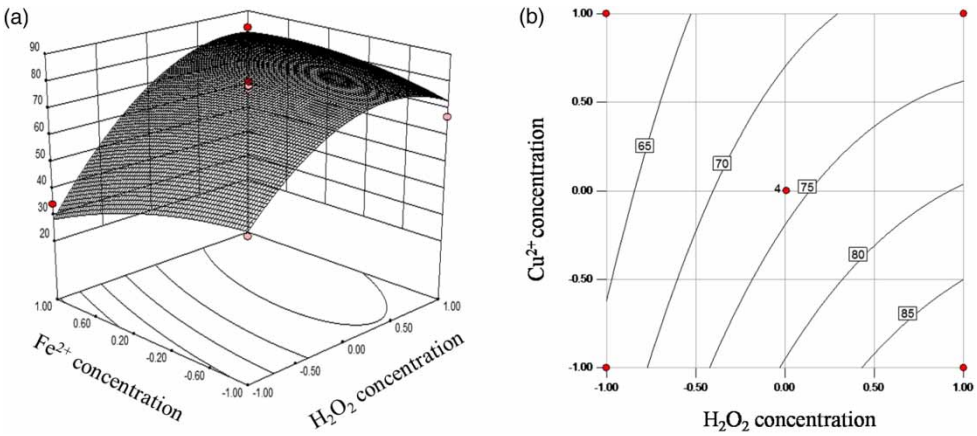

Figure 3 | (a) 3D response surface plot of TOC removal using UV Fe-Fenton and (b) 2D plot using UV Cu-Fenton as a function of Fe^{2+} or Cu^{+} and H_2O_2 dosage (coded values as in Table S2, available online) at pH 3 and using 375 W of UV lamp.

constant UV irradiation intensity. Therefore, the optimized reaction parameters obtained from RSM are 176 mM H_2O_2 and 9.6 mM Fe^{2+} using 500 W UV lamp for UV-Fe-Fenton process, and 276 mM H_2O_2 and 2.95 mM Cu^{2+} using 480 W UV lamp for UV-Cu-Fenton process. The predicted TOC removal efficiency is 96% for both systems.

Radicals identification and catalytic mechanism in UV-Fe/Cu-Fenton oxidation

ESR spectroscopy was used to clarify the Cl^- effect on the generation of radicals during the UV-Fenton reaction. As shown in Figure 4(a) and 4(c), DMPO-·OH adduct was the only species observed for UV-Fe-Fenton system in aqueous solution with and without NaCl addition, the intensity of DMPO-·OH was moderately inhibited by Cl^- ions (Moffett & Zika 1987; De Laat *et al.* 2004; Machulek *et al.* 2007). It should be noted that the $HO_2\cdot/O_2\cdot^-$ may also contribute to the DMPO-·OH adducts signal, since DMPO-·OOH/$\cdot O_2^-$ adducts readily decays into DMPO-·OH in aqueous solution (Houriez *et al.* 2010). Accordingly, excess amount of methanol was used as the reaction matrix to examine the $HO_2\cdot/O_2\cdot^-$. As shown in Figure 4(d), DMPO-·OOH or DMPO-$\cdot O_2^-$ adducts were detected, indicating the generation of ·OOH or $\cdot O_2^-$ radicals (Bosnjakovic & Schlick 2006). When NaCl was added with methanol as solvent, almost no signal was detected at all (Figure 4(b)), revealing the inhibitive effect of NaCl on $HO_2\cdot/O_2\cdot^-$ formation. Without NaCl, UV irradiation could promote the reduction of Fe(III)-aqua complexes as Equation (9) and generate superoxide radicals, however, in the presence of NaCl, the reduction of Fe(III)-Cl complexes occurred (Equation (11)). The calculation results in Table 1 show that ·OH radicals were dominant reactive oxygen species (ROS) in the saline water. All these evidences suggested that the generation of $HO_2\cdot/O_2\cdot^-$ from Fe^{3+} catalyzed H_2O_2 decomposition was inhibited in hypersaline water, due to the complexation of Cl^- with Fe^{3+}, and thus the ·OH play a crucial role in organics oxidation.

Figure 5 shows the ESR spectra of DMPO-radical adducts formed in UV-Cu-Fenton system. DMPO-·OH adducts were observed for Cu ions catalyzed H_2O_2 decomposition in aqueous solution (Figure 5(a) and 5(c)), and the intensity of ·OH was greatly decreased and the signal shifted to lower magnetic field with addition of NaCl, indicating the suppression of ·OH generation besides scavenging of ·OH by Cl^- ions differently with UV-Fe-Fenton. The nine peaks in Figure 5(b) assigned to DMPO-·O_2^- (marked with *) or DMPO-·O_2H adduct (marked with o) and other oxygen-centered radical adducts (marked with Δ), respectively (Kohno *et al.* 1994; Bosnjakovic & Schlick 2006). The dominant ROS are superoxide radicals in the presence of NaCl and methanol (Figure 5(b)). However, without NaCl, the multiple peaks in Figure 5(d) suggests a lower content of DMPO-·O_2^- or DMPO-·O_2H adducts (Table 1). The six peaks with hyperfine coupling constants $a_N = 14$ G and $a_H = 11$ G could be attributed to the DMPO-$\cdot O_2^-$ or DMPO-·O_2H adducts (marked with ♣ and •), the peaks marked with ♦ and □ ($a_N = 13.5$ G and $a_H = 9$ G) were from DMPO-·OCH_3 adduct, and the three peaks marked with √ were from the degradation product of DMPO (Bosnjakovic & Schlick 2006). Therefore, it could be deduced that the $HO_2\cdot/O_2\cdot^-$ are more important than OH· in the UV-Cu-Fenton reaction, especially with the addition of NaCl, compared with the Fe-Fenton system.

Moreover, it was noted that the color of the reaction medium of UV-Cu-Fenton system changed from blue to yellow and finally returned to blue, indicating the disappearing

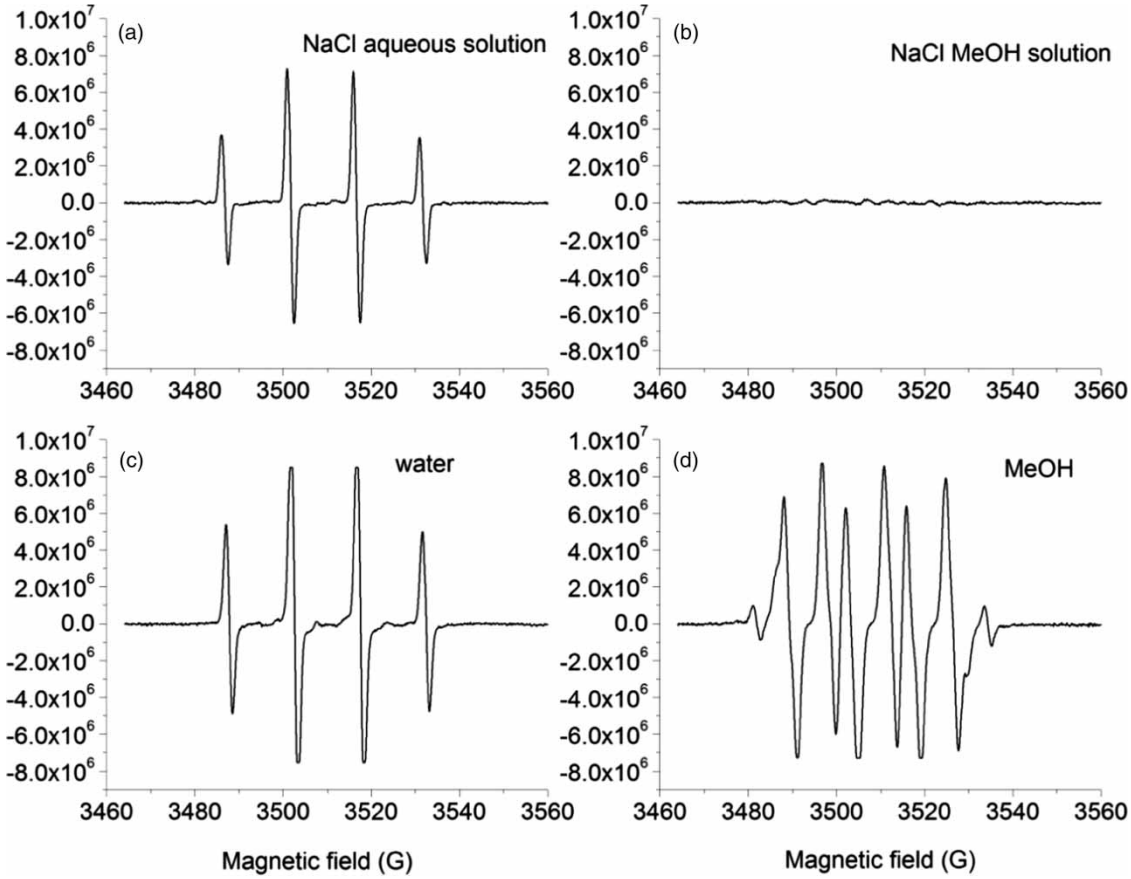

Figure 4 | ESR spectra of DMPO-radical adducts of UV-Fe-Fenton reaction in (a) 20% w/v NaCl solution and (c) pure water, (b) 20% w/v NaCl solution in methanol matrix and (d) methanol without NaCl. Experiments in each graph were conducted under identical instrument parameters. $[Fe^{2+}]_0 = 5$ mmol/L, $[H_2O_2]_0 = 0.1$ mol/L.

Table 1 | Semi-quantitative analysis of the radicals generated using the highest ESR peak intensity

Peak intensity		·OH ($\times 10^6$)	O_2· ($\times 10^6$)	·OH/ O_2·
UV-Fe-Fenton	without Cl^-	8.49	8.58	0.99
	with Cl^-	7.30	0.11	66
UV-Cu-Fenton	without Cl^-	0.76	0.40	1.9
	with Cl^-	0.22	0.45	0.49

of Cu-aqua complexes $Cu(H_2O)_4^{2+}$ and formation of CuOH or Cu-peroxide (Perez-Benito 2004; Lan *et al.* 2016). The formed Cu-peroxide intermediates could be decomposed to Cu(I) and $O_2{\cdot}^-$ under UV irradiation (Lan *et al.* 2016). The formation of Cu^+ was confirmed by XPS analysis of the Cu-sludge after reaction (Figure S6 in the Supplementary Material, available online).

Feasibility analysis of UV-Fe/Cu-Fenton reaction

The formation of iron (hydr)oxides precipitates on the UV lamp was a serious problem for UV assisted Fenton reaction, by which the catalytic efficiency decreased after running several times. However, there was no scaling on UV lamp in UV-Cu-Fenton system, due to the formation of cupric salts other than hydroxides (Figure S7, available online). In addition, the formed iron (hydr)oxides precipitates cannot be reused easily and had to be treated as hazardous sludge. However, the cupric salt catalyst could be reused by precipitation, filtration and re-dissolution. Moreover, according to the optimization results from RSM, less amount of Cu^{2+} was need than Fe^{2+} to get adequate removal of TOC from the studied wastewater. Therefore, UV-Cu-Fenton is more promising for efficient mineralization of hypersaline wastewater from epoxy resin production.

CONCLUSION

Hypersaline wastewater with high concentration of organic contaminants is a challenge for effective treatment. The high salinity of wastewater significantly inhibited the oxidation

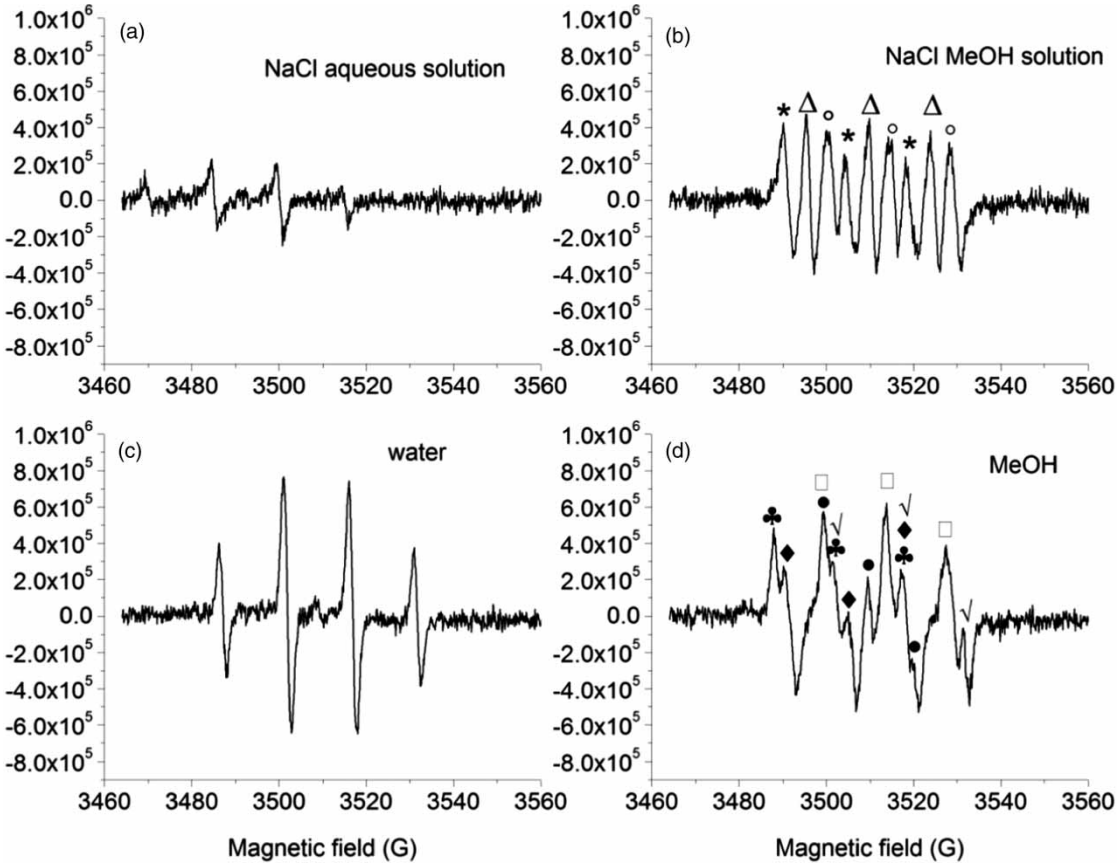

Figure 5 | ESR spectra of DMPO-radical adducts of UV-Cu-Fenton reaction in (a) 20% w/v NaCl aqueous solution and (c) pure water, (b) 20% w/v NaCl solution in methanol matrix and (d) methanol without NaCl. Experiments in each graph were conducted under identical instrument parameters. $[Cu^{2+}]_0 = 5$ mmol/L, $[H_2O_2]_0 = 0.1$ mol/L.

efficiency of the organic pollutants, and the high TOC restrains the reuse of inorganic salts. Therefore, enhanced mineralization of hypersaline wastewater should be considered in the advanced treatment to provide a possibility for salt resources recovery. The UV assisted Fe^{2+} catalyzed and Cu^{2+} catalyzed Fenton oxidation of hypersaline wastewater both are efficient for TOC removal of hypersaline resin processing wastewater. Continuous dosing of Fenton's reagent and pH maintenance at 3 is beneficial for the Fe^{2+} catalyzed Fenton oxidation. With the use of RSM, the operation parameters were optimized as 176 mM H_2O_2 and 9.6 mM Fe^{2+} using 500 W UV lamp for UV-Fe-Fenton process, and 276 mM H_2O_2 and 2.95 mM Cu^{2+} using 480 W UV lamp for UV-Cu-Fenton process. The predicted TOC removal efficiency could reach 96% for both systems. However, the catalytic mechanisms involving radicals were different for UV-Fe-Fenton and Cu-Fenton reaction. Hydroxyl radical was dominant oxidant in UV-Fe^{2+}-Fenton process, while $HO_2\cdot/O_2\cdot^-$ played a more important role in the UV-Cu-Fenton system. Moreover, no scaling or sludge problem makes UV-Cu-Fenton a promising alternative method for efficient mineralization of hypersaline industrial wastewater.

ACKNOWLEDGEMENTS

This work was financially supported by the National Natural Science Foundation of China (Grant Nos 21577160, 51338010 and 51290282).

REFERENCES

Bokare, A. D. & Choi, W. 2014 Review of iron-free Fenton-like systems for activating H_2O_2 in advanced oxidation processes. *Journal of Hazardous Materials* **275**, 121–135.

Bosnjakovic, A. & Schlick, S. 2006 Spin trapping by 5,5-dimethylpyrroline-*N*-oxide in Fenton media in the presence of Nafion perfluorinated membranes: limitations and

potential. *Journal of Physical Chemistry B* **110** (22), 10720–8.

De Laat, J., Truong Le, G. & Legube, B. 2004 A comparative study of the effects of chloride, sulfate and nitrate ions on the rates of decomposition of H_2O_2 and organic compounds by Fe(II)/H_2O_2 and Fe(III)/H_2O_2. *Chemosphere* **55** (5), 715–723.

Duesterberg, C. K. & Waite, T. D. 2006 Process optimization of Fenton oxidation using kinetic modeling. *Environmental Science and Technology* **40** (13), 4189–4195.

Eisenberg, G. M. 1943 Colorimetric determination of hydrogen peroxide. *Industrial and Engineering Chemistry Analytical Edition* **15**, 327–328.

Gallard, H., De Laat, J. & Legube, B. 1999 Comparative study of the rate of decomposition of H_2O_2 and of atrazine by Fe(III)/H_2O_2, Cu(II)/H_2O_2, Fe(III)/Cu(II)/H_2O_2. *Journal of Water Science* **12** (4), 713–728.

Giri, A. S. & Golder, A. K. 2014 Fenton, photo-Fenton, H_2O_2 photolysis, and TiO_2 photocatalysis for dipyrone oxidation: drug removal, mineralization, biodegradability, and degradation mechanism. *Industrial & Engineering Chemistry Research* **53** (4), 1351–1358.

Houriez, C., Ferré, N., Siri, D., Tordo, P. & Masella, M. 2010 Structure and spectromagnetic properties of the superoxide radical adduct of DMPO in water: elucidation by theoretical investigations. *Journal of Physical Chemistry B* **114** (36), 11793–11803.

Kohno, M., Mizuta, Y., Kusai, M., Masumizu, T. & Makino, K. 1994 Measurements of superoxide anion-radical and superoxide anion scavenging activity by electron-spin-resonance spectroscopy coupled with DMPO spin-trapping. *Bulletin of the Chemical Society of Japan* **67** (4), 1085–1090.

Lan, S. Y., Xiong, Y., Tian, S. H., Feng, J. X. & Xie, T. Y. 2016 Enhanced self-catalytic degradation of CuEDTA in the presence of H_2O_2/UV: evidence and importance of Cu-peroxide as a photo-active intermediate. *Applied Catalysis B-Environmental* **183**, 371–376.

Lipczynskakochany, E., Sprah, G. & Harms, S. 1995 Influence of some groundwater and surface waters constituents on the degradation of 4-chlorophenol by the Fenton reaction. *Chemosphere* **30** (1), 9–20.

Machulek, A. J., Moraes, J. E. F., Vautier-Giongo, C., Silverio, C. A., Friedrich, L. C., Nascimento, C. A. O., Gonzalez, M. C. & Quina, F. H. 2007 Abatement of the inhibitory effect of chloride anions on the photo-Fenton process. *Environmental Science and Technology* **41** (24), 8459–8463.

Maciel, R., Sant'Anna, G. L. & Dezotti, M. 2004 Phenol removal from high salinity effluents using Fenton's reagent and photo-Fenton reactions. *Chemosphere* **57** (7), 711–719.

Millero, F. J., Johnson, R. L., Vega, C. A., Sharma, V. K. & Sotolongo, S. 1992 Effect of ionic interactions on the rates of reduction of Cu(II) with H_2O_2 in aqueous solutions. *Journal of Solution Chemistry* **21** (12), 1271–1287.

Moffett, J. W. & Zika, R. G. 1987 Reaction kinetics of hydrogen peroxide with copper and iron in seawater. *Environmental Science and Technology* **21** (8), 804–810.

Nadtochenko, V. & Kiwi, J. 1998 Photoinduced mineralization of xylidine by the Fenton reagent. 2. Implications of the precursors formed in the dark. *Environmental Science & Technology* **32** (21), 3282–3285.

Nerud, F., Baldrian, P., Gabriel, J. & Ogbeifun, D. 2001 Decolorization of synthetic dyes by the Fenton reagent and the Cu/pyridine/H_2O_2 system. *Chemosphere* **44** (5), 957–961.

Nieto-Juarez, J. I., Pierzchła, K., Sienkiewicz, A. & Kohn, T. 2010 Inactivation of MS2 coliphage in Fenton and Fenton-like systems: role of transition metals, hydrogen peroxide and sunlight. *Environmental Science and Technology* **44** (9), 3351–3356.

Peng, J. B., Li, J. H., Shi, H. H., Wang, Z. Y. & Gao, S. X. 2016 Oxidation of disinfectants with Cl-substituted structure by a Fenton-like system Cu^{2+}/H_2O_2 and analysis on their structure-reactivity relationship. *Environmental Science and Pollution Research* **23** (2), 1898–1904.

Perez-Benito, J. F. 2004 Reaction pathways in the decomposition of hydrogen peroxide catalyzed by copper(II). *Journal of Inorganic Biochemistry* **98** (3), 430–438.

Pignatello, J. J. 1992 Dark and photoassisted iron(3+)-catalyzed degradation of chlorophenoxy herbicides by hydrogen peroxide. *Environmental Science and Technology* **26** (5), 944–951.

Pignatello, J. J., Oliveros, E. & MacKay, A. 2006 Advanced oxidation processes for organic contaminant destruction based on the Fenton reaction and related chemistry. *Critical Reviews in Environmental Science and Technology* **36** (1), 1–84.

Salazar, R., Brillas, E. & Sires, I. 2012 Finding the best Fe^{2+}/Cu^{2+} combination for the solar photoelectro-Fenton treatment of simulated wastewater containing the industrial textile dye Disperse Blue 3. *Applied Catalysis B-Environmental* **115**, 107–116.

Tang, W. Z. & Huang, C. P. 1996 2,4-dichlorophenol oxidation kinetics by Fenton's reagent. *Environmental Technology* **17** (12), 1371–1378.

Teel, A. L., Warberg, C. R., Atkinson, D. A. & Watts, R. J. 2001 Comparison of mineral and soluble iron Fenton's catalysts for the treatment of trichloroethylene. *Water Research* **35** (4), 977–984.

Wang, J. L. & Xu, L. J. 2012 Advanced oxidation processes for wastewater treatment: formation of hydroxyl radical and application. *Critical Reviews in Environmental Science and Technology* **42** (3), 251–325.

Wei, L., Zhu, H., Mao, X. H. & Gan, F. X. 2011 Electrochemical oxidation process combined with UV photolysis for the mineralization of nitrophenol in saline wastewater. *Separation and Purification Technology* **77** (1), 18–25.

Wu, C. H., Wu, J. T. & Lin, Y. H. 2016 Mineralization of sulfamethizole in photo-Fenton and photo-Fenton-like systems. *Water Science and Technology* **73** (4), 746–750.

First received 7 May 2018; accepted in revised form 27 August 2018. Available online 6 September 2018